Semaphorin3a regulates endothelial cell number and podocyte differentiation during glomerular development

Kimberly J. Reidy[1], Guillermo Villegas[1], Jason Teichman[1], Delma Veron[2], Wa Shen[1], Juan Jimenez[3], David Thomas[4] and Alda Tufro[2,*]

Semaphorin3a (Sema3a), a chemorepellant guidance protein, plays crucial roles in neural, cardiac and peripheral vascular patterning. Sema3a is expressed in the developing nephron, mature podocytes and collecting tubules. Sema3a acts as a negative regulator of ureteric bud branching, but its function in glomerular development has not been examined. Here we tested the hypothesis that Sema3a regulates glomerular vascular development using loss- and gain-of-function mouse models. Sema3a deletion resulted in defects in renal vascular patterning, excess endothelial cells within glomerular capillaries, effaced podocytes with extremely wide foot processes and albuminuria. Podocyte Sema3a overexpression during organogenesis resulted in glomerular hypoplasia, characterized by glomerular endothelial cell apoptosis, delayed and abnormal podocyte foot process development, a complete absence of slit diaphragms and congenital proteinuria. Nephrin, WT1 and VEGFR2 were downregulated in Sema3a-overexpressing kidneys. We conclude that Sema3a is an essential negative regulator of endothelial cell survival in developing glomeruli and plays a crucial role in podocyte differentiation in vivo. Hence, a tight regulation of Sema3a dosage is required for the establishment of a normal glomerular filtration barrier.

KEY WORDS: Semaphorin, Glomerular development, Podocyte differentiation, Endothelial cell migration, Mouse

INTRODUCTION

Glomerulogenesis requires spatially directed cell migration, cell differentiation and modulation of cell-cell and cell-matrix interactions to generate the tri-layered structure of the mature glomerular filter. The signaling mechanisms that guide these processes are not fully understood (Quaggin and Kreidberg, 2008). Vascular endothelial growth factor (VEGFA) induces vasculogenesis and stimulates endothelial cell proliferation and migration into the vascular cleft of S-shaped bodies to form glomerular capillaries (Eremina et al., 2003; Gerber et al., 1999; Kitamoto et al., 1997; Tufro, 2000; Tufro et al., 1999). As capillaries form, adjacent epithelial cells envelop the capillary loop and differentiate into podocytes, forming foot processes and slit diaphragms (SDs) that replace the immature cell-cell interactions [occluding junctions (OJ)]. Gene deletion studies have identified several proteins (including nephrin, podocalyxin, LMX1β, POD1, podocin, kreisler and GLEPP1) that are required to establish podocyte foot processes and slit diaphragms, although the mechanisms involved are unclear. Recruitment of mesangial cells into the developing vascular tuft is dependent upon endothelial cell secretion of platelet-derived growth factor B (Lindahl et al., 1998). Together, podocytes and endothelial cells synthesize the glomerular basement membrane (GBM) and assemble the tri-layered glomerular filtration barrier (Abrahamson et al., 1998; Sariola, 1984). Major GBM components, such as laminin α5, form a structural framework for glomerular development, and both laminin α5 and its receptor α3 integrin are required for glomerulogenesis (Kreidberg et al., 1996; Miner and Li, 2000).

Semaphorin3a (Sema3a) is a chemorepellent with multiple guidance functions, including axon pathfinding, cardiac and peripheral vascular patterning and branching morphogenesis. Sema3a gene deletion results in perinatal lethality (Behar et al., 1996). Sema3a signaling is mediated by a complex of the binding receptor neuropilin 1 and the signaling receptors plexinA1 or A3 (He and Tessier-Lavigne, 1997; Kolodkin et al., 1997; Tamagnone et al., 1999). Both Sema3a and its receptor neuropilin 1 are expressed in the developing glomerulus, and Sema3a remains expressed in adult podocytes and collecting tubules (Robert et al., 2000; Villegas and Tufro, 2002). Sema3a inhibits ureteric bud branching by downregulation of glial-cell-line-derived neurotrophic factor (Tufro et al., 2008). The function of Sema3a during glomerular development is unknown. In cultured podocytes, recombinant SEMA3A downregulates podocin expression, decreases the interaction between SD proteins podocin, nephrin and CD2AP and induces podocyte apoptosis through inhibition of the phosphorylation of AKT (Guan et al., 2006). Moreover, administration of recombinant SEMA3A to wild-type mice induces foot process effacement and fusion, endothelial cell swelling and reversible albuminuria, representing a novel mechanism for proteinuria (Tapia et al., 2008).

We hypothesized that Sema3a plays a role in the formation of the glomerular filtration barrier. We examined the effect of Sema3a gene dosage on glomerular filter development using loss- and gain-of-function models. Here we show that Sema3a gene deletion causes defective renal vascular patterning, excess endothelial cells and poor glomerular capillary lumen development, whereas podocyte Sema3a overexpression during kidney organogenesis leads to glomerular hypoplasia, glomerular endothelial apoptosis and abnormal podocyte differentiation with a complete absence of slit diaphragms. Thus, a tightly regulated Sema3a dosage is required for the development of a normal glomerular filtration barrier.

[1]Department of Pediatrics, [3]Imaging Facility, and [4]Department of Pathology, Albert Einstein College of Medicine, Bronx, NY, USA. [2]Department of Pediatrics, Yale University School of Medicine, 333 Cedar Street, New Haven, CT 06520-8064, USA.

*Author for correspondence (alda.tufro@yale.edu)

MATERIALS AND METHODS

All experiments were performed in accordance with approved protocols and AECOM Institute of Animal Studies regulations. Mice were housed in a pathogen-free environment.

Sema3a-null mutant mice

Sema3a$^{+/-}$ mice (Behar et al., 1996) were bred and their progeny (*n*=31) were examined at birth. *Sema3a*$^{+/-}$ mice were bred with *Flk1-lacZ*$^{+/-}$ mice (Shalaby et al., 1995). Progeny from *Flk1-lacZ*$^{+/-}$: *Sema3a*$^{+/-}$ mice were examined at birth (*n*=29). Mice were genotyped using appropriate PCR primers (Behar et al, 1996; Shigehara et al, 2003); for *tet-O-Sema3a*, the primers 5′-TTAGTGAACCGTCAGATCGCC-3′ and 5′-CAGCCCAC-TTGCATTCATCTC-3′ were used. *Flk1-lacZ*$^{+/-}$ mice were identified by *lacZ* staining (Lobe et al., 1999).

Generation of podocyte-specific Sema3a-overexpressing mice

Sema3a cDNA (NM_017310) was cloned into the *Mlu1* and *Nhe1* sites of pBI-EGFP (Clontech) carrying the Tet-responsive promoter (Tet-On System). *TetO-Sema3a* mice were generated by pronuclear injection of DNA into FVB embryos (Transgenic Facility, AECOM) and were bred with *podocin-rtTA* mice (Shigehara et al., 2003) to yield bi-transgenic *podocin-rtTA: tetO-Sema3a* mice. Isolated glomeruli were used to confirm *Sema3a* transgene induction. Glomeruli were isolated from adult *podocin-rtTA: tetO-Sema3a* mice and single transgenics induced with doxycycline for 7 days, and un-induced *podocin-rtTA: tetO-Sema3a* mice (*n*=4 per group), using a reported protocol (Takemoto et al., 2006). *Sema3a* mRNA was measured by qPCR as described below.

Pregnant bi-transgenic dams were fed doxycycyline (625 mg/kg feed, Harlan-Teklad, Madison, WI, USA) from embryonic day 12 (E12) until birth (NB1) or 2 weeks of age. Doxycycline dosing was started at E12 to allow for therapeutic doxycycline levels to be reached by the onset of podocin expression in the developing embryos at E14. *Podocin-rtTA: tet-O-Sema3a* progeny were examined at both NB1 and 2 weeks of age and were compared with induced single-transgenic littermates and with age-matched un-induced *podocin-rtTA: tet-O-Sema3a* as controls.

Cells

Mouse glomerular endothelial cells (MGEC) were isolated from *Flk1-lacZ*$^{+/-}$ mice as previously described (Tufro-McReddie et al., 1997; Tufro, 2000). Endothelial cells were cloned and characterized by immunocytochemistry, β-Gal and Fluorescent Lectin stainings. Primary antibodies used were anti-Flk1 (sc-315, Santa Cruz), anti-CD31 (Pharmingen), anti-α smooth muscle actin clone 1A4 (#A2547, Sigma) and anti-WT1 (sc-192, Santa Cruz).

Migration assays

MGEC/Kidney co-culture

Cell Tracker-labeled MGEC were co-cultured with embryonic kidneys (E12) and exposed for 24 hours to either media plus 250 ng/ml rat recombinant *Sema3a* or media plus vehicle. MGEC migration towards the explants was examined 12 and 24 hours later by phase- and confocal microscopy (Olympus Fluoview FV300).

Quantitative migration assay

5×10^3 MGEC were plated on 8 μm pore filters (Nunc, 137443) in complete MGEC media and allowed to attach for 1 hour, starved for 1 hour in serum-free media. Serum-free media, with or without recombinant SEMA3A (500 ng/ml), was added in the lower chamber, and cells were incubated at 37°C for 6 hours. At the end of the experiment, cells on the upper side of the insert were mechanically removed, and the cells on the lower side of the insert were fixed in 10% buffered formalin for 25 minutes, stained with 0.1% Crystal Violet for 30 minutes, then counted. Experiments were performed in duplicate and repeated four times.

Immunoblotting

Kidneys were lysed in a modified radio immuno precipitation assay (RIPA) buffer (Karihaloo et al., 2005). Pooled samples of whole kidney lysates were generated using equal micrograms of protein from each mouse. Proteins were resolved by 8-15% SDS-PAGE and immunoblotting was performed using standard western blotting technique with the following primary antibodies: anti-WT1 (Santa Cruz, sc192, 1:200); anti-nephrin (Fitzgerald, 1:500); anti-podocin (gift from Peter Mundel, 1:500); anti-CD2AP (Santa Cruz, sc-9137, 1:200); anti-PAX2 (Zymed, 71-6000, 1:250); anti-VEGF (Santa Cruz, sc507, 1:200); anti-VEGFR2 (Santa Cruz, sc-315, 1:500); anti-neuropilin 1 (gift from Alex Kolodkin, 1:1000); and anti-actin (Sigma, A2066, 1:1000). To assess albuminuria, equal volumes of urine were resolved on SDS-PAGE and immunoblotted with anti-BSA antibody (Upstate, 07-248, 1:1000).

Immunohistochemistry (IHC)

Freshly harvested kidneys were either fixed in 10% formalin for 24 hours and embedded in paraffin or incubated in 18% sucrose for 10 minutes, embedded in optimal cutting temperature (OCT) compound and frozen in isopentane mixed with dry ice. Cryosections were fixed in –20°C acetone (or 4% paraformaldehyde for PAX2/synaptopodin IHC), permeabilized with 0.3% Triton-X, and blocked in 2-5% donkey serum, 1% BSA, 0.1% gelatin, 0.1% Triton-X, 0.05% Tween and 0.05% sodium azide. For the WT1/anti-activated caspase 3 dual-immunostaining, sections from paraffin-embedded, formalin-fixed kidneys were rehydrated, microwaved in citrate buffer (pH 6.0) and blocked as above. For F4/80 IHC, antigen retrieval was with proteinase K, with detection by Vectastain ABC kit and DAB (Vector Labs). The following primary antibodies and dilutions were used: anti-cleaved caspase 3 (Cell Signaling, 1:300), anti-CD31 (BD Pharmingen, 1:50), anti-F4/80 (eBioscience, 1:100), anti-nephrin (Fitzgerald, 1:500), anti-PAX2 (Zymed, 1:25), anti-PCNA (Santa Cruz, 1:50), anti-podocin (1:50) and anti-NT-synaptopodin (gifts from P. Mundel, 1:200), and anti-WT1 (Dako, 1:50). Secondary antibodies were fluorescent-tagged donkey Cy2 and Cy3 (Jackson ImmunoResearch Laboratories, Pennsylvania, USA). Confocal images were obtained (Olympus Fluoview 300/ Leica AOBS). For negative controls, primary antibodies were omitted.

Quantitative real-time PCR (qPCR)

Total RNA was isolated from whole kidney tissue using Trizol Reagent (Invitrogen) as per the manufacturer's instructions or from isolated glomeruli using RNeasy Minikit (Qiagen). 1 μg of isolated RNA from each animal was used to generate cDNA (Qiagen Quantitect kit). PCR reactions used individually isolated glomeruli cDNA or pooled cDNA [*Sema3a*$^{-/-}$ and *Sema3a*$^{+/+}$, *n*=7 mice per group; *podocin-rtTA; tet-O-Sema3a* newborns –dox (doxycycline) and +dox, *n*=6 mice per group], and amplification was performed using Applied Biosystems SYBR-Green Mastermix with an Eppendorf Realplex² Mastercycler. PCR primers were designed with Primer Express software and were as follows [the melting temperature (Tm) of each primer pair is shown in parentheses]:

Sema3a (60°C), 5′-GGATGGGTCCTCATGCTCAC-3′ (forward) and 5′-TGGTGCTGCAAGTCAGAGCAG-3′ (reverse);

Sema3b (58°C), 5′-TCCTGCACCTCCTGGCC-3′ (forward) and 5′-ACCAACTGCAGAAAGTCCCG-3′ (reverse);

Sema3c (60°C), 5′-GGACATGGGCTGGCTCTGT-3′ (forward) and 5′-GGATGTCCTTTGGATGGAAGG-3′ (reverse);

Sema3d (58°C), 5′-ACCATCGCTGGGGTGCAATAT-3′ (forward) and 5′-GGGTGCCGCCTTATGAAAC-3′ (reverse);

Sema3e (58°C), 5′-AGGATTCTCTGTCCTCCCATGTC-3′ (forward) and 5′-AGGCCCCACTATCAATGG-3′ (reverse);

Sema3f (60°C), 5′-AGGGCCCCAACTATCAATGG-3′ (forward) and 5′-CATCAGGGTAGTCCTTAGTGGACTTC-3′ (reverse);

Sema3g (60°C), 5′-ACTTGCACCACTCTGGAACATG-3′ (forward) and 5′-GGCAAAACGGACCACGG-3′ (reverse);

Gapdh (58-60°C), 5′-GCATGGCCTTCCGTGTTCCTA-3′ (forward) and 5′-GCCGCCTGCTTCACCACCTTCT-3′ (reverse);

ubiquitin (60°C), 5′-GCCCAGTGTTACCACCAGAAG-3′ (forward) and 5′-GCTCTTTTTAGATACTGTGGTGAGGAA-3′ (reverse).

PCR products were amplified using following protocol: 95°C for 10 minutes; followed by 45 cycles of Tm for 1 minute, 95°C for 15 seconds. Reactions were run in duplicate and each experiment was repeated three times. Gene expression relative to housekeeping genes *Gapdh* or ubiquitin was determined with the $2^{-\Delta\Delta Ct}$ method (Schmittgen and Livak, 2008).

Terminal deoxynucleotidyl transferase biotin-dUTP nick end labeling (TUNEL)

Apoptotic nuclei were identified using In Situ Cell Death Detection Kits (Chemicon) following the manufacturer's protocol. Detection was performed by either immunoperoxidase-DAB, counterstained with Periodic Acid Schiff (PAS), or fluorescein-conjugated anti-digoxigenin, followed by application of rhodamine-labeled *Griffonia simplicifolia* Lectin I (Vector Labs; 1:150) to label endothelial cells (Laitinen, 1987). Apoptotic cells were counted in each glomerulus of the kidney sections (n=4-5 mice per group, mean=25 glomeruli per mouse).

Transmission electron microscopy (TEM)

For TEM, the kidney cortex was fixed with 2% paraformaldehyde and 2.5% glutaraldehyde in 0.1 M sodium cacodylate buffer, post-fixed with 1% osmium tetroxide followed by 1% Uranyl Acetate, dehydrated and embedded in LX112 resin (LADD Research Industries, Burlington, VT, USA). Ultrathin (80 nm) sections were cut on a Reichert Ultracut UCT, stained with Uranyl Acetate followed by Lead Citrate and viewed on a JEOL 1200EX transmission electron microscope at 80 kv.

Histologic and TEM morphometric analysis

Kidney sections were stained with PAS solution and glomerular volume was determined by measuring the diameters of all glomeruli within three sections. Glomerular volume was calculated as $Gv=\beta/k\cdot(\pi\cdot r^2)^{3/2}$, where β=1.38 is the shape coefficient for spheres, k=1.1 is the size distribution coefficient and $(\pi\cdot r^2)$ is the glomerular area (Hirose et al., 1982). To determine glomerular endothelial cell number in *Sema3a* mutant mice, endothelial cell nuclei were identified in 1-3 capillary loops per mouse on 5000× TEM images of *Sema3a*$^{+/+}$ and *Sema3a*$^{-/-}$ mice. Image J software (NIH) was used to determine the number of cell-cell interactions per µm of GBM (pore density) and foot process width, and to quantify WT1 and CD31 images (n=3 kidneys per group, 15-40 glomeruli per section). The total GBM length examined per group was: *Sema3a*$^{+/+}$, 58,064 nm; Sema3a$^{-/-}$, 117,842 nm; newborn *podocin-rtTA: tet-O-Sema3a* mice (–dox), 156,312 nm; newborn *podocin-rtTA: tet-O-Sema3a* mice (+dox), 95,477 nm; 2-week-old pups (–dox), 190,808 nm; 2-week-old pups (+dox), 167,516 nm.

Statistical analysis

Student's unpaired *t*-test was used to compare groups. *P*<0.05 was deemed statistically significant.

RESULTS

Sema3a loss-of-function results in renal vascular defects

To define the effect of *Sema3a* deletion on glomerular development we compared kidneys from newborn *Sema3a*$^{-/-}$ and *Sema3a*$^{+/+}$ mice histologically and by TEM. Light microscopy examination of *Sema3a*$^{-/-}$ glomeruli revealed poor capillary lumen development and increased nuclei within the loops, whereas *Sema3a*$^{+/+}$ glomeruli had normal wide-open capillary loops (Fig. 1A). On examination with TEM, *Sema3a*$^{+/+}$ mice had open glomerular capillaries with fenestrated endothelium, podocyte foot processes linked by SDs and a normal GBM (Fig. 1B). By contrast, TEM revealed significant abnormalities in *Sema3a*$^{-/-}$ glomeruli. There was no visible capillary lumen in *Sema3a*$^{-/-}$ glomeruli, even in the most mature glomeruli, and multiple endothelial cells were visualized within the capillary loops (Fig. 1B). Fenestrae were absent in these abnormal endothelial cells. Morphometric analysis of TEM images showed that *Sema3a*$^{-/-}$ glomeruli had twice the number of endothelial cells per capillary loop as compared with *Sema3a*$^{+/+}$ glomeruli (Fig. 1C). The GBM appeared morphologically normal in *Sema3a*$^{-/-}$ newborn mice. However, many podocyte foot processes were extremely wide and linked by OJs rather than SDs (Fig. 1B). Quantification of these abnormalities demonstrated a broad variation in podocyte foot process width in *Sema3a*$^{-/-}$ glomeruli, with some foot processes 30-fold wider than the average width of *Sema3a*$^{+/+}$ foot processes, whereas others were only 1.5-fold wider or normal (Fig. 1B,C). Remarkably, the morphologic abnormalities in the glomerular endothelium and foot process development of *Sema3a*$^{-/-}$ mice were associated with impaired glomerular filtration barrier function as evidenced by albuminuria on immunoblotting (Fig. 1D).

The defects in glomerular capillary formation suggested the possibility of more-widespread patterning defects. To define the vascular phenotype resulting from *Sema3a* gene deletion, we bred *Sema3a*$^{+/-}$ mice (Behar et al., 1996) with *Flk1-lacZ*$^{+/-}$ knock-in mice (Shalaby et al., 1995), and generated double-heterozygotes *Flk1-lacZ*$^{+/-}$: *Sema3a*$^{+/-}$ (see Table S1 in the supplementary material).
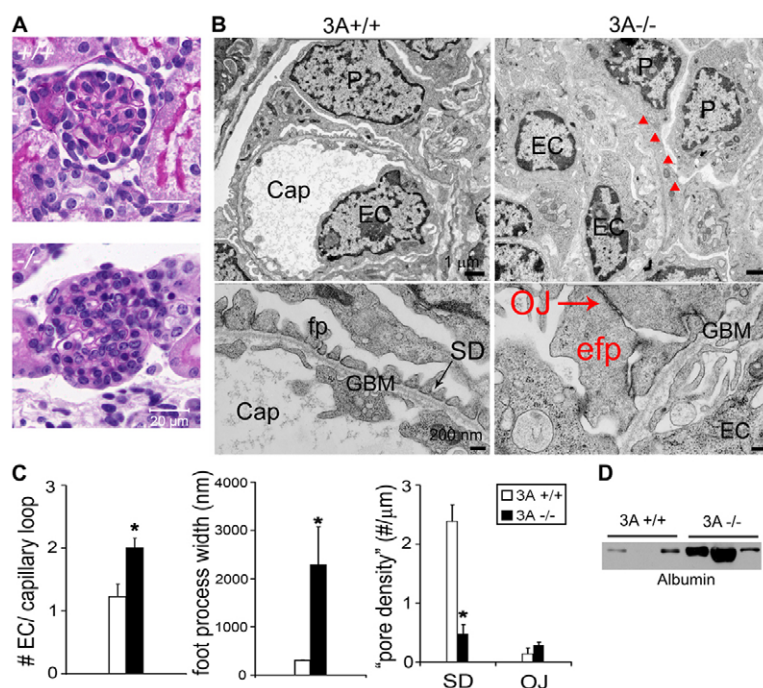

Fig. 1. *Sema3a* deletion results in excess glomerular endothelial cells and podocyte foot process effacement. (**A**) PAS-stained wild-type glomerulus (+/+) with open capillaries; *Sema3a*-null (–/–) glomerulus shows multiple blue nuclei in the capillary loops and few open lumina. (**B**) TEM: newborn *Sema3a*$^{+/+}$ (3A+/+) glomeruli demonstrate intact foot processes (fp), slit diaphragms (SDs), GBM and endothelial cells (EC). *Sema3a*$^{-/-}$ (3A–/–) glomeruli show multiple EC within the capillary loop, wide foot processes (efp: effaced foot process, red arrowheads) joined by occluding-junctions (OJ). P, podocyte; Cap, capillary lumen. (**C**) TEM morphometric analysis: the number of EC per capillary loop is two-fold higher, the foot processes are ~seven-fold wider, and the SD density is five-fold lower in *Sema3a*$^{-/-}$ glomeruli versus wild-type glomeruli (n=8 mice per group, *P*=0.0002). *, *P*<0.05. (**D**) Western blot showing albuminuria in *Sema3a*$^{-/-}$ newborn mice. Scale bars: in A, 20 µm; in B, 1 µm for upper panel, 200 nm in lower panel.
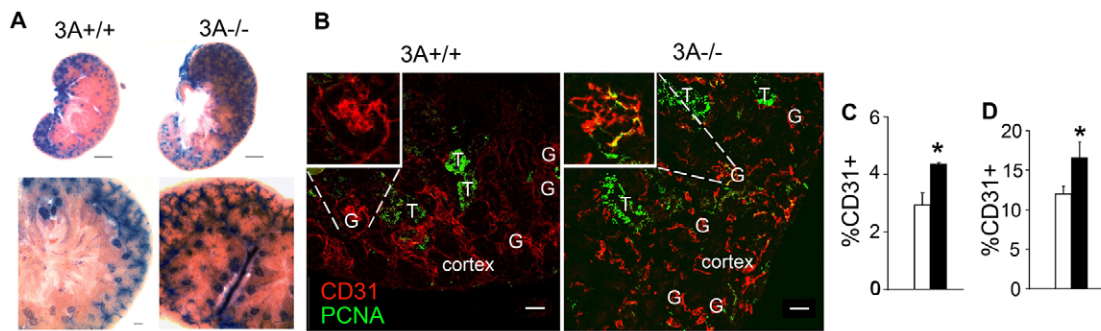
Fig. 2. *Sema3a* deletion causes excess renal endothelial cells and disrupts vascular patterning. (**A**) β-Gal-stained kidney sections (80 μm thick) from newborn progeny of *Flk1/lacZ⁺/⁻: Sema3a⁺/⁻* mice. In wild-type (3A+/+) kidneys, most Flk1-positive endothelial cells localize to the cortex; *Sema3a⁻/⁻* (3A–/–) kidneys show abnormal renal vascular patterning, and increased endothelial cells can be observed throughout. (**B**) Newborn kidneys with endothelial cells immunostained for CD31 (red) and proliferating cells for PCNA (green) showing that most proliferation localizes to tubules (T) in both *Sema3a⁺/⁺* and *Sema3a⁻/⁻* newborn mice. Insets: higher magnification of glomeruli (G) with endothelial cell proliferation (yellow) exclusively in *Sema3a⁻/⁻* mice. (**C,D**) Quantification of CD31 immunostaining confirming increased cortical and glomerular endothelial cells in *Sema3a⁻/⁻* kidneys: (C) proportion of CD31-positive cortical area (%); (D) proportion of CD31-positive glomerular area (%). *, *P*<0.05. Scale bars: in A, 200 μm for upper panel, 50 μm for lower panel; in B, 25 μm.

Kidneys from the newborn progeny of *Flk1-lacZ⁺/⁻: Sema3a⁺/⁻* were stained for *lacZ* to examine renal endothelial cell patterning (Fig. 2A). *Flk1-lacZ⁺/⁻: Sema3a⁻/⁻* kidneys exhibited increased *Flk1*-positive cells throughout in a disorganized pattern, indicating an abnormal number and distribution of endothelial cells with loss of *Sema3a* function (Fig. 2A). To confirm the vascular phenotype, endothelial cells were immunostained with anti-CD31 antibody. *Sema3a⁻/⁻* kidneys had a 50% increase in cortical CD31-positive immunofluorescence as compared with *Sema3a⁺/⁺* kidneys, confirming a global excess of renal endothelial cells in *Sema3a⁻/⁻* mice (Fig. 2B,C). Congruent with the findings of increased glomerular endothelial cells on TEM, the CD31-positive area within *Sema3a⁻/⁻* glomeruli was 38% larger than the CD31-positive area within *Sema3a⁺/⁺* glomeruli (Fig. 2D).

Excess glomerular endothelial cells could be the result of increased endothelial cell proliferation, decreased endothelial cell apoptosis or increased endothelial cell migration. Dual-label immunostaining with anti-CD31 and anti-PCNA antibodies was performed to identify endothelial and proliferating cells, respectively. PCNA staining in both *Sema3a⁺/⁺* and *Sema3a⁻/⁻* newborn kidneys localized predominantly to tubules and not in glomeruli. Proliferating endothelial cells were rarely observed within glomeruli and the nephrogenic cortex and occurred in less than 1% of the total cortical area (Fig. 2B), suggesting that the majority of endothelial cells were not proliferating in newborn *Sema3a⁻/⁻* kidneys.

Previous in vitro studies indicated that *Sema3a* negatively regulates cell survival (Bagnard et al., 2001; Guan et al., 2006; Guttmann-Raviv et al., 2007; Moretti et al., 2008). Apoptotic cells, identified by either TUNEL or immunodetection of cleaved caspase 3, were scarce in newborn glomeruli (Fig. 3A,B). Although no difference in overall apoptotic rate could be detected between *Sema3a⁻/⁻* and *Sema3a⁺/⁺* glomeruli, co-localization of TUNEL-positive cells and endothelial cells labeled by *Griffonia simplicifolia* Lectin (Laitinen, 1987) demonstrated a five-fold decrease in glomerular endothelial apoptotic rate in *Sema3a* mutants (0.05±0.02 vs 0.01±0.01 endothelial apoptotic cells per glomeruli, in *Sema3a⁺/⁺* and *Sema3a⁻/⁻*, respectively, *P*<0.05). This suggests that decreased endothelial apoptosis contributes to the excess endothelial cells observed in *Sema3a⁻/⁻* kidneys. Next,

we examined *Sema3a* effects on glomerular endothelial cell migration using in vitro assays (Tufro, 2000). Recombinant SEMA3A decreased glomerular endothelial cell migration across membranes and towards embryonic kidneys (Fig. 3C-E; also see Fig. S1 in the supplementary material), suggesting that *Sema3a* acts as a chemorepellant and impairs glomerular endothelial cell migratory response to chemoattractant stimuli. Collectively, in vivo and in vitro data suggest that loss of *Sema3a* promotes endothelial cell survival and migration, respectively, resulting in an excess of renal endothelial cells and renal vascular patterning defects.

Sema3a and its receptors are expressed in macrophages and induce apoptosis (Ji et al., 2009). Thus, we examined whether *Sema3a* loss-of-function altered macrophage number in the kidney using F4/80 IHC. No F4/80-positive cells were identified in glomeruli of either *Sema3a⁻/⁻* or *Sema3a⁺/⁺* kidneys (see Fig. S2 in the supplementary material). Interstitial macrophages were present, but F4/80-positive cell counts in *Sema3a⁻/⁻* and *Sema3a⁺/⁺* kidneys were similar [10±1.3 vs 10.3±0.7 F4/80-positive cells per 400× field, in *Sema3a⁻/⁻* and *Sema3a⁺/⁺*, respectively, *P*=not significant (ns)].

Sema3a deletion alters PAX2 expression in the developing kidney

We next examined the expression levels of VEGFA and its receptors VEGFR2 and neuropilin 1 in *Sema3a⁻/⁻* mice (Fig. 4). Wild-type and *Sema3a⁻/⁻* kidneys had similar levels of expression of both VEGFA and its receptors, suggesting that the renal vascular phenotype occurring upon *Sema3a* deletion was not due to upregulation of VEGFA but rather to an imbalance between VEGFA and *Sema3a* signaling pathways. To explore further the abnormalities underlying the glomerular phenotype observed in *Sema3a* mutant mice, we examined the expression of podocyte-specific proteins and transcription factors relevant to podocyte differentiation. We determined that nephrin, podocin and WT1 expression was unchanged, whereas PAX2 expression was decreased by 30% in *Sema3a⁻/⁻* mice (Fig. 4). Localization of WT1, synaptopodin and PAX2 by immunofluorescence was not altered in *Sema3a⁻/⁻* kidneys (Fig. 3B, also see Fig. S3A in the supplementary material).
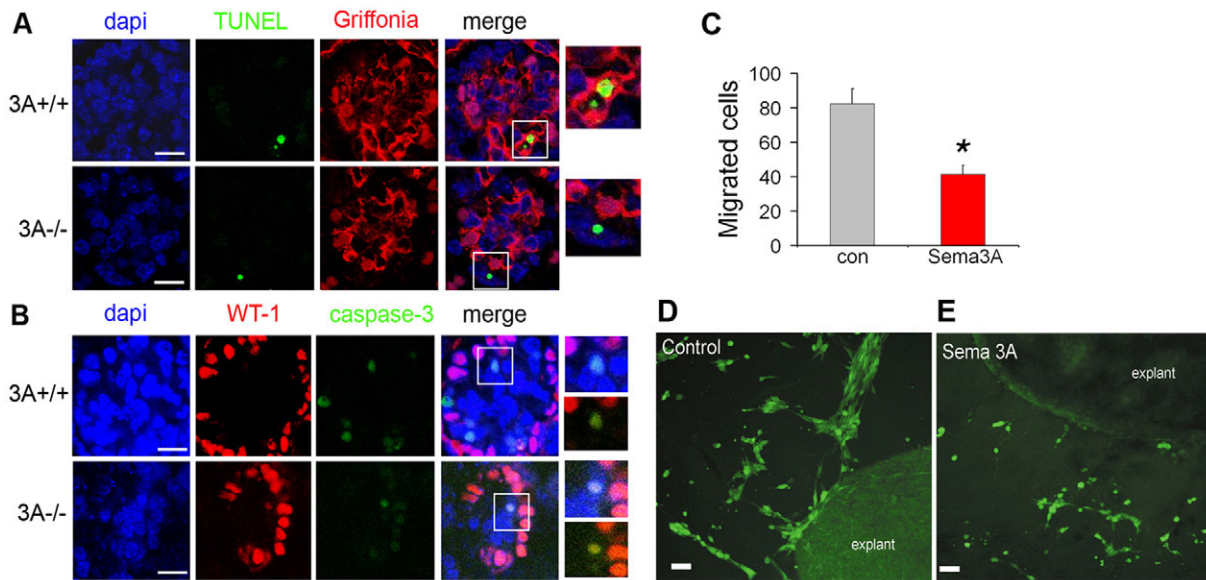
Fig. 3. Loss of *Sema3a* promotes glomerular endothelial survival and migration. (**A**,**B**) Glomerular apoptosis detected by TUNEL assay (A) and by cleaved caspase 3 immunofluorescence (B) is shown; insets show apoptotic nuclei at higher magnification, nuclei are labeled with DAPI (blue). Merge between WT1 and DAPI appears pink, demonstrating nuclear WT1 staining. (A) In *Sema3a*$^{+/+}$ glomeruli, apoptotic nuclei (green) co-localize with *Griffonia simplicifolia* Lectin I-labeled endothelium (red), indicating endothelial cell apoptosis (yellow in merged images), whereas no apoptotic endothelial cells were detected in the representative *Sema3a*$^{-/-}$ glomerulus shown. (B) Apoptotic cells were rare in both *Sema3a*$^{-/-}$ and *Sema3a*$^{+/+}$ glomeruli, most *Sema3a*$^{+/+}$ apoptotic nuclei (green) were not WT1-positive podocytes, and most *Sema3a*$^{-/-}$ apoptotic nuclei (green) were WT1-positive podocytes (yellow in merge). (**C**) Quantitative migration assay showing that *Sema3a* decreases mouse endothelial cell migration (MGEC) by approximately 50%. Data are expressed as mean ± s.e.m. of four experiments. *, $P<0.05$. (**D**,**E**) *Sema3a* blunts embryonic kidney chemo-attraction for MGEC. (D) Co-culture of embryonic kidneys with MGEC showing MGEC migrating towards the explant (control). (E) Co-culture of embryonic kidneys with MGEC exposed to Sema3a (250 ng/ml) prevented MGEC migration towards the explant (Sema3A). Scale bars: in A, 10 μm; in B, 10 μm; in D,E, 50 μm.

Sema3a gain-of-function during nephrogenesis impairs podocyte differentiation

To define further the function of *Sema3a*, we examined the effects of podocyte *Sema3a* overexpression during kidney organogenesis in vivo using an inducible tetracycline-regulated model (Tet-On). *Tet-O-Sema3a* transgenic mice were generated as described in the Material and methods and were bred with *podocin-rtTA* mice (Shigehara et al., 2003). Uninduced *podocin-rtTA: tet-O-Sema3a* mice have normal life spans, are fertile and have normal size litters. Following a one-week induction with doxycycline, adult *podocin-rtTA: tet-O-Sema3a* mice exhibited a four-fold higher *Sema3a* mRNA level in isolated glomeruli as compared with controls (Fig. 5A). Controls included single transgenic mice on doxycycline and uninduced *podocin-rtTA: tet-O-Sema3a* mice.

Podocin-rtTA: tet-O-Sema3a mice were induced from E12 until either birth or two weeks after birth, at completion of nephrogenesis (see Table S1 in the supplementary material). Controls were single transgenic littermates and age-matched uninduced *podocin-rtTA: tet-O-Sema3a* mice. Mice overexpressing *Sema3a* during kidney organogenesis exhibited smaller glomeruli at birth, with a 30% decrease in mean glomerular volume (Fig. 5B,C). On examination with TEM, glomeruli from control newborns exhibited fully differentiated podocyte foot processes linked by SDs, a fenestrated endothelium and a normal newborn GBM (Fig. 5D). In contrast, glomeruli from *Sema3a*-overexpressing mice had immature, cuboidal podocytes that lacked differentiated foot processes (Fig. 5D) and extended flat and wide processes (~six-fold wider than those of uninduced controls; Fig. 5E). In contrast to the variable podocyte abnormalities observed in *Sema3a*$^{-/-}$ glomeruli, the

podocyte processes of glomeruli from *Sema3a*-overexpressing mice were uniformly flat and extremely wide. Their immaturity was further demonstrated by the complete absence of SDs, with adjacent processes being solely joined by OJs (Fig. 5E). There was a decrease in total cell-cell interaction density (pore density), as the number of OJs did not compensate for the lack of SDs (Fig. 5E). In addition, glomerular endothelial cells of newborn *Sema3a*-overexpressing
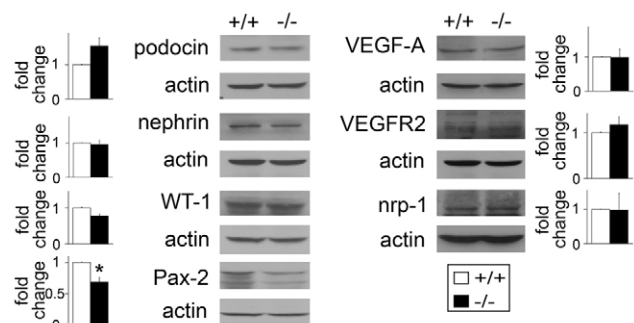

Fig. 4. *Pax2* is downregulated in *Sema3a*$^{-/-}$ kidneys. Western blots showing *Pax2* downregulation in *Sema3a*$^{-/-}$ versus *Sema3a*$^{+/+}$ kidneys. Nephrin, podocin, WT1, VEGFA, VEGFR2 and neuropilin 1 (nrp-1) expression was similar in *Sema3a*$^{-/-}$ and wild-type kidneys. Representative immunoblots of pooled samples (*n*=5 mice per genotype) are shown; bar graphs show densitometric analysis, expressed as fold change ± s.e.m. (*n*≥3), *Sema3a*$^{-/-}$ versus *Sema3a*$^{+/+}$, corrected for actin. *, $P<0.05$.
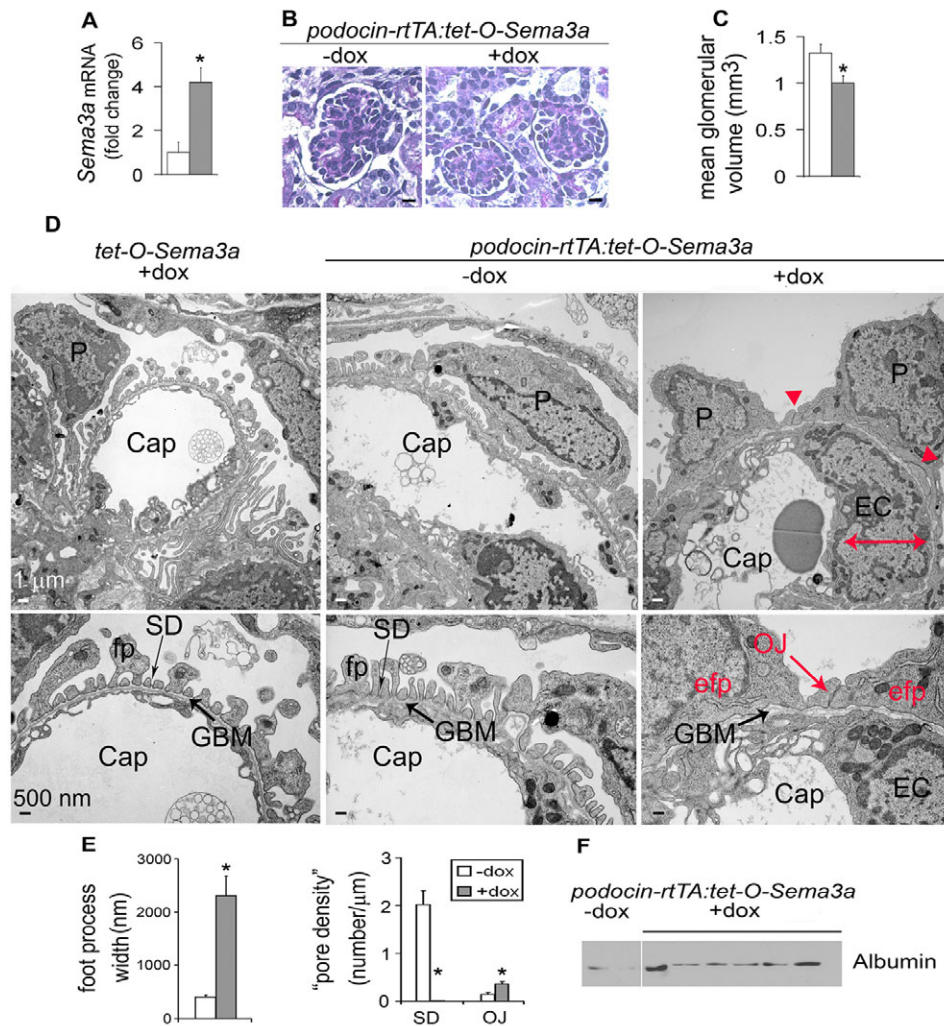
Fig. 5. Overexpression of podocyte *Sema3a* results in glomerular hypoplasia, undifferentiated podocytes and congenital proteinuria. (**A**) qPCR showing four-fold upregulation of *Sema3a* mRNA in isolated glomeruli of adult mice overexpressing *Sema3a* (gray bar), after a one-week induction with doxycycline versus controls (white bar, uninduced *podocin-rtTA: tet-O-Sema3a* and *tet-O-Sema3a* or *podocin-rtTA* on doxycyline). Data were normalized to ubiquitin and expressed as a fold-change from controls (*n*=4 per group, *, *P*<0.05). (**B,C**) PAS staining (B) demonstrating smaller glomeruli in newborn *Sema3a*-overexpressing (+dox) mice induced during kidney organogenesis. Glomerular volume (C) is decreased in *Sema3a*-overexpressing mice (gray bars) versus controls (white bars), *n*=4 per group. *, *P*<0.05. (**D**) TEM images demonstrating immature cuboidal podocytes (P) linked by occluding junctions (OJ) instead of slit diaphragms (SD) in newborn *Sema3a*-overexpressing mice induced during organogenesis (+dox). The endothelial cell (EC) appears swollen (red double-headed arrows) in induced glomeruli. Uninduced age-matched mice (–dox) and single transgenic littermates exhibit intact podocyte foot processes (fp) with normal GBM and fenestrated endothelium. Cap: capillary lumen, efp: effaced foot process (red arrowheads). (**E**) TEM morphometric analysis showing significantly wider foot processes (effacement), slit diaphragm absence and increase in occluding-junction number in *Sema3a*-overexpressing kidneys. *, *P*<0.05. (**F**) Western blot showing albuminuria in *Sema3a*-overexpressing mice (+dox) vs controls (–dox). Scale bars: in B, 10 μm; in D, 1 μm for upper panel, 500 nm for lower panel.

mice were swollen and vacuolated, with decreased fenestrations, whereas the GBM appeared morphologically similar to that seen in control newborns (Fig. 5D).

The absence of foot processes and SDs observed in newborn *Sema3a*-overexpressing mice could represent *Sema3a*-mediated impairment of foot process and SD formation or a developmental delay. Hence, we examined *Sema3a*-overexpressing mice at completion of nephrogenesis. Two-week-old control glomeruli exhibited normal podocyte foot processes with SDs, GBM and fenestrated endothelium as described in the newborn (Fig. 6A). By contrast, TEM images from two-week-old *Sema3a*-overexpressing glomeruli revealed incompletely differentiated and abnormal

podocyte foot processes. Foot processes from two-week-old *Sema3a*-overexpressing kidneys were flat and 50% wider than age-matched controls (Fig. 6A,B). Strikingly, these processes failed to form SDs and were joined by OJs (Fig. 6A). Glomerular endothelial cells remained swollen and had decreased fenestration, whereas the GBM was morphologically normal (Fig. 6A).

The dramatic defects in podocyte differentiation and endothelial cell damage induced by podocyte *Sema3a* gain-of-function during organogenesis were associated with altered glomerular permselectivity. Albuminuria was evident on immunoblotting both in newborn (Fig. 5F) and two-week-old (Fig. 6C) *Sema3a*-overexpressing mice. Collectively, these
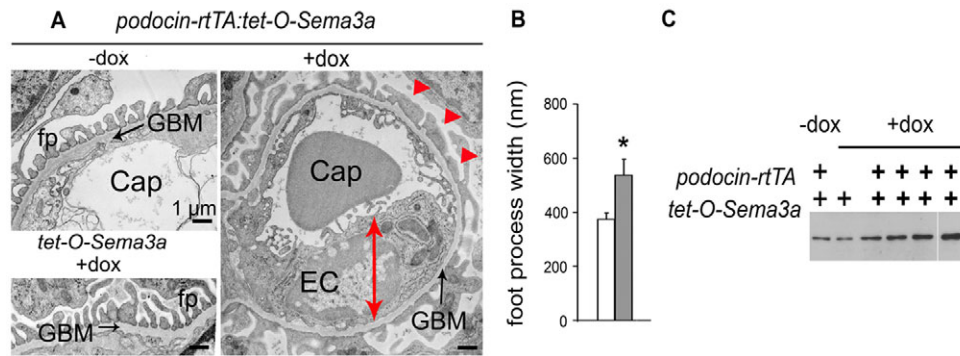
DEVELOPMENT

Fig. 6. Podocyte foot process development is delayed and abnormal in mice overexpressing podocyte *Sema3a*. (**A**,**B**) TEM: *Sema3a*-overexpressing (+dox) glomeruli at completion of nephrogenesis (2 weeks) have wide podocyte foot processes (arrowheads) and absent slit diaphragms; a morphometric analysis is shown in B. Note that the endothelial cells (EC) are swollen (double-headed arrow). Controls (–dox) exhibit intact podocyte foot processes (fp), normal GBM and fenestrated endothelium. Cap: capillary lumen. (**C**) Urine albumin immunoblot demonstrates albuminuria in 2-week-old induced *Sema3a*-overexpressing mice (+dox), which is absent in controls (–dox). Scale bars: 1 μm.

findings indicate that podocyte *Sema3a* plays a crucial role in podocyte differentiation and SD formation during glomerular development.

To investigate the molecular mechanism underlying the undifferentiated podocyte phenotype, we next examined expression of SD proteins. Nephrin expression decreased to half of normal levels in *Sema3a*-overexpressing kidneys, as determined by immunoblotting and confirmed by immunofluorescence (Fig. 7A,B). By contrast, podocin expression was unchanged, suggesting that the decrease in nephrin expression was not due to loss of podocytes (Fig. 7A,B). The expression level of the adaptor protein, CD2AP, was also not altered by *Sema3a* overexpression (Fig. 7A). Furthermore, *Sema3a*-

overexpressing mice had a greater than 50% decrease in WT1 expression in comparison with controls (Fig. 7A). A decrease in the intensity of the nuclear WT1 staining in *Sema3a*-overexpressing glomeruli as compared with controls was also observed, although the podocyte cell count was unchanged (Fig. 8D,E).

Synaptopodin immunostaining demonstrated similar patterns of expression in *Sema3a*-overexpressing and control kidneys, as reported in another model of abnormal podocyte differentiation (Miner et al., 2002) (see Fig. S3 in the supplementary material). Thus, despite their morphologic immaturity as observed on TEM, *Sema3a*-overexpressing podocytes were capable of expressing cytoskeletal, but not SD markers characteristic of mature podocytes.
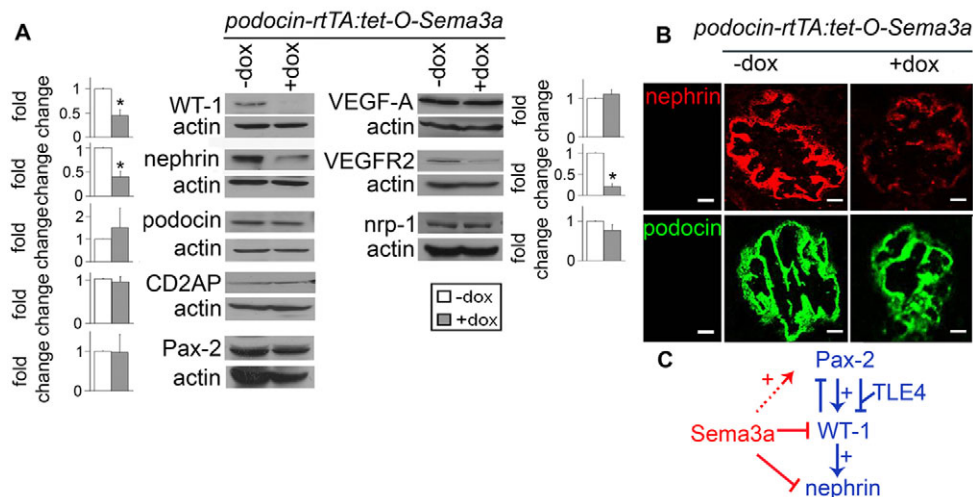

Fig. 7. Podocyte *Sema3a* overexpression downregulates nephrin, WT1 and VEGFR2. (**A**) Immunoblots showing nephrin, WT1 and VEGFR2 downregulation in *Sema3a*-overexpressing mice (+dox E12 to 2 weeks of age). Representative blots and densitometric analysis of three separate experiments are shown; data are expressed as fold change ± s.e.m. after correction for actin; +dox vs –dox were compared using pooled samples of *n*=13-20 mice per group; *, *P*<0.05. (**B**) Immunostaining demonstrating that nephrin expression is decreased in newborn *Sema3a*-overexpressing glomeruli (+dox), whereas podocin expression is unchanged. (**C**) Proposed model of the *Sema3a* effect on PAX2 and WT1 signaling. Previously described pathways are shown in blue: PAX2 is capable of either upregulation or repression of WT1 expression, depending upon the absence or presence, respectively, of the transcriptional co-repressor groucho TLE4. WT1 stimulates nephrin expression, and it downregulates PAX2 through a negative-feedback loop. The effects of *Sema3a* on these pathways are shown in red: *Sema3a* negatively regulates WT1 and nephrin and might positively regulate PAX2. Therefore, upon *Sema3a* deletion, PAX2 expression is downregulated, and, upon *Sema3a* overexpression, WT1 and nephrin expression is decreased.
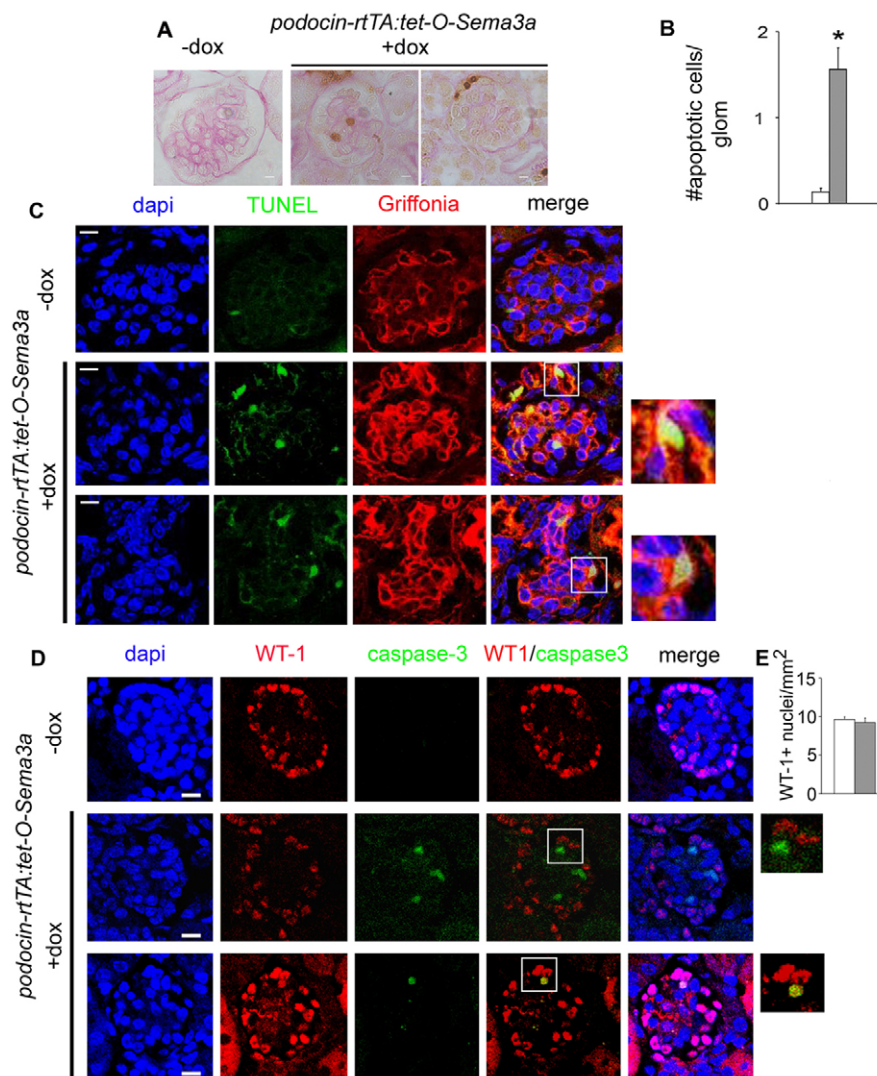
Fig. 8. Podocyte *Sema3a* overexpression negatively regulates glomerular endothelial cell survival, and podocyte number is not changed. (**A**) Several apoptotic nuclei (brown) identified by TUNEL in *Sema3a*-overexpressing glomeruli (+dox) versus virtually none in controls (–dox). (**B**) Quantification showing an eight-fold increase in apoptotic nuclei per glomerulus in *Sema3a*-overexpressing mice (gray bar) versus controls (white bar). *, $P<0.05$. (**C,D**) Identification of apoptotic cell type is shown by TUNEL assay and EC labeling (C) or by activated-caspase-3 immunofluorescence and podocyte labeling (D); nuclei are labeled with DAPI (blue). (C) In *Sema3a*-overexpressing glomeruli (+dox), apoptotic nuclei (green) co-localize with *Griffonia simplicifolia* Lectin I-labeled endothelium (red), indicating endothelial cell apoptosis (yellow in merged images; insets show apoptotic nuclei at a higher magnification). Two representative glomeruli are shown. (D) WT1 (red) and activated caspase 3 (green) immunostaining. Control glomeruli (–dox) show WT1-positive podocytes and no apoptosis (negative for activated caspase 3). Two representative glomeruli from *Sema3a*-overexpressing mice (+dox) are shown. In most glomeruli, apoptotic nuclei are WT1-negative (top inset), indicating that the apoptotic cells are not podocytes. Only 10% of apoptotic cells were deemed to be podocytes (WT1-positive and caspase-3-positive, shown in yellow, bottom inset). (**E**) Podocyte number quantification (WT1-positive nuclei per mm^2 glomerular area) showing similar podocyte numbers in controls (white bar) and *Sema3a*-overexpressing mice (gray bar). $n=40$-100 glomeruli per group; $P=$ns. Scale bars: in C, 5 μm; in D, 10 μm.

The localization and expression level of the immature nephron transcription factor PAX2, known to downregulate WT1 and nephrin (Cai et al., 2003; Wagner et al., 2006), was normal in *Sema3a*-overexpressing kidneys (Fig 7A; also see Fig. S3 in the supplementary material). Together, these data suggest that the phenotype observed in *Sema3a*-overexpressing kidneys is not secondary to podocyte loss and that excess *Sema3a* regulates podocyte differentiation downstream of PAX2 by downregulating WT1 and nephrin (Fig. 7C).

Podocyte *Sema3a* overexpression during organogenesis did not alter renal VEGFA and neuropilin 1 expression levels (Fig. 7A). By contrast, *Sema3a*-overexpressing mice demonstrated a 75% reduction in expression of renal VEGFR2 as compared with controls (Fig. 7A), suggesting that the effects on podocyte phenotype might in part be mediated by decreased VEGF signaling.

Sema3a is a negative regulator of glomerular endothelial and epithelial cell survival

Sema3a negatively regulates cell survival in vitro (Guan et al., 2006; Guttmann-Raviv et al., 2007). Thus, we examined if *Sema3a* overexpression induced apoptosis in vivo by TUNEL assay. Newborn *Sema3a*-overexpressing glomeruli exhibited an 8-fold increase in apoptotic cells as compared with controls (Fig. 8A,B).

The vast majority (95%) of TUNEL-positive nuclei in *Sema3a*-overexpressing glomeruli co-localized with the endothelial marker *Griffonia simplicifolia* Lectin I (Fig. 8C). Thus, *Sema3a* overexpression during organogenesis enhanced glomerular endothelial cell apoptosis in vivo. Next, we examined the effect of *Sema3a* overexpression on podocyte survival in vivo: podocytes were identified by WT1 and apoptotic cells were identified using activated caspase-3 immunofluorescence. Congruent with the TUNEL assay data, *Sema3a* overexpression increased glomerular cell apoptosis (mean: 1.2±0.43 activated caspase-3-positive nuclei per *Sema3a*-overexpressing glomeruli vs 0.3±0.09 positive nuclei per control glomeruli, $P<0.05$). The majority of apoptotic cells identified in *Sema3a*-overexpressing mice were not WT1-positive (Fig. 8D); however, six out of 46 (13%) apoptotic nuclei did co-localize with WT1, indicating that *Sema3a* does induce some podocyte apoptosis in vivo. To exclude the possibility of podocyte dropout, podocyte number per glomerular cross-section was measured by WT1 immunostaining. There was no significant difference between *Sema3a*-overexpressing glomeruli and controls (9.6±0.3 vs 9.2±0.6 podocytes per mm^2 of glomerular area, in *Sema3a*-overexpressing mice vs controls, respectively $P=$ns; Fig. 8D). Thus, the predominant cell type undergoing apoptosis in *Sema3a*-overexpressing kidneys is the glomerular endothelial cell.

A small number of podocytes in *Sema3a*-overexpressing mice were also undergoing apoptosis, but this did not result in net podocyte loss (Fig. 8E).

Compensatory changes in class 3 semaphorin gene expression

Redundant functions among class 3 semaphorins have been reported in multiple cell types (Guttmann-Raviv et al., 2007). Thus, we asked whether expression levels of other class 3 semaphorins are altered in developing *Sema3a*$^{-/-}$ kidneys. Real-time PCR showed a two-fold increase in *Sema3e* mRNA expression in *Sema3a*$^{-/-}$ as compared with *Sema3a*$^{+/+}$ kidneys, whereas expression of *Sema3b*, *3c*, *3d* and *3g* was unchanged (see Fig. S4 in the supplementary material). *Sema3a* was downregulated to minimal levels in *Sema3a*$^{-/-}$ kidneys, as expected (see Fig. S4 in the supplementary material). By contrast, podocyte *Sema3a* overexpression resulted in a 2.8-fold upregulation of *Sema3b* expression, and no change in total kidney *Sema3a*, *3c*, *3d*, *3e* or *3g* was identified as compared with controls (see Fig. S4 in the supplementary material).

DISCUSSION

Sema3a loss- and gain-of-function studies in mice demonstrated that a tightly regulated *Sema3a* gene dosage is necessary for normal glomerular development and glomerular filtration barrier function.

Sema3a acts as a negative regulator of endothelial cell survival and migration during kidney organogenesis

Sema3a deletion increased renal endothelial cell number and altered renal vascular patterning. The glomerular endothelial cell increase resulted from reduced apoptosis. *Sema3a* inhibited endothelial cell migration in migration assays, consistent with previous reports (Guttmann-Raviv et al., 2007; Miao et al., 1999; Serini et al., 2003). Glomerular capillary development involves both vasculogenesis and angiogenesis, and podocyte VEGFA provides chemo-attractive signals that direct glomerular endothelial cell migration (Abrahamson et al., 1998; Eremina et al., 2003; Tufro-McReddie et al., 1997; Tufro, 2000; Tufro et al., 1999). *Sema3a* deletion did not alter kidney VEGFA, neuropilin 1 or VEGFR2, suggesting that *Sema3a* does not regulate their expression level. *Sema3a* is known to compete with VEGFA for binding to neuropilin 1 and probably acts as a gatekeeper for endothelial cells (Bagnard et al., 2001; Miao et al., 1999). Hence, in the *Sema3a*-null kidneys, unopposed VEGFA signaling might have contributed to the abnormalities of vascular patterning.

Neuropilin-1-deficient mice phenocopy *Sema3a*$^{-/-}$ mutants and exhibit lethal defects in neural and cardiovascular patterning; conversely, overexpression of neuropilin 1 results in embryonic lethality owing to an excess of capillary formation (Kawasaki et al., 1999; Kitsukawa et al., 1995). However, recently the role of *Sema3a* in vascular development has been called into question by reports of no obvious large vessel defects in mice expressing a mutant neuropilin 1 incapable of binding to *Sema3a*, and a recent study that failed to replicate vascular defects described in *Sema3a*$^{-/-}$ mice (Gu et al., 2003; Vieira et al., 2007). Notably, these studies did not examine the kidney vasculature.

Predictably, newborn mice overexpressing podocyte *Sema3a* did not have abnormal capillary development, given that the gain-of-function occurred after E14.5 when most of the vascular patterning had already been established. Endothelial cell apoptosis was induced by podocyte *Sema3a* gain-of-function, as revealed by TEM and TUNEL analysis, indicating that *Sema3a* participates in the crosstalk between these cell types by a non-cell-autonomous mechanism.

Increased glomerular endothelial cell apoptosis was reported in mice overexpressing podocyte angiopoietin 2, associated with VEGFA downregulation (Davis et al., 2007). Taken together, our data suggest that *Sema3a* negatively regulates endothelial cell survival during glomerular development and that a tight regulation of *Sema3a* dosage is necessary for normal glomerular vascularization.

Sema3a regulates podocyte differentiation

Remarkably, *Sema3a* deletion results in abnormal podocyte morphology despite normal expression levels of SD proteins. This suggests that the podocyte phenotype in *Sema3a*$^{-/-}$ mice might be secondary to aberrant crosstalk between the podocytes and endothelial cells, as has been proposed in other models of endothelial injury (Eremina et al., 2003). However, given that podocyte development occurs in metanephric cultures in the absence of glomerular capillary formation, and that *Sema3a* receptors are present in podocytes (Avner et al., 1988; Guan et al., 2006; Harper et al., 2001), the abnormal podocyte structure might also represent a *Sema3a* cell-autonomous requirement for normal podocyte differentiation. Interestingly, transcription factor PAX2 was downregulated in *Sema3a*$^{-/-}$ newborn mice. Deletion of the *Pax2* gene results in complete renal agenesis and prevents mesenchymal-epithelial transition (Torres et al., 1995), and, although the degree of downregulation was mild and was not sufficient to impair nephron induction, it suggests that, during kidney development, *Sema3a* signaling might impact a fundamental pathway required for epithelial differentiation.

Gain-of-function studies provided strong evidence for a role of *Sema3a* in podocyte differentiation. The complete absence of SDs and the congenital proteinuria observed in mice overexpressing *Sema3a* in podocytes are reminiscent of mice deficient in nephrin and the clinical correlate congenital nephrotic syndrome (Kestila et al., 1998; Putaala et al., 2001). Moreover, the undifferentiated podocyte morphology in mice overexpressing *Sema3a* is associated with downregulation of WT1, nephrin and VEGFR2, indicating that *Sema3a* signaling impacts major podocyte signaling pathways and structural proteins (Done et al., 2008). Dominant-negative and loss-of-function mutations in *Wt1* have been identified in infantile nephrotic syndrome associated with Denys-Drash and Frasier syndromes (Little et al., 1995). *Wt1* knockout mice exhibited downregulation of nephrin and diffuse mesangial sclerosis, similar to patients with Denys-Drash, indicating that the transcription factor WT1 is a regulator of nephrin expression and is required for proper podocyte differentiation (Guo et al., 2002). Together, the data suggest that the undifferentiated podocyte phenotype observed in *Sema3a*-overexpressing mice is a consequence of the downregulation of WT1 and nephrin. Downregulation of WT1 and nephrin, in association with glomerular hypoplasia and proteinuria, was also noted in mice with inappropriate *Pax2* expression post-natally (Wagner et al., 2006); however, no change in *Pax2* expression was found in mice overexpressing *Sema3a*. PAX2 signaling is complex: PAX2 can activate WT1 expression (Dehbi et al., 1996; McConnell et al., 1997), but, in the presence of the transcriptional co-repressor groucho TLE4, the opposite occurs, and WT1 expression is repressed (Cai et al., 2003; Wagner et al., 2006). WT1, in turn, is a positive regulator of nephrin expression (Guo et al., 2004; Wagner et al., 2004) and a negative regulator of PAX2 through a feedback loop (Ryan et al., 1995). Collectively, downregulation of WT1 and nephrin by *Sema3a* overexpression, and downregulation of PAX2 in *Sema3a*$^{-/-}$ mice, suggest that *Sema3a* might function as a modifier of PAX2 and WT1 signaling during podocyte differentiation (Fig. 7C). Thus, *Sema3a* may act as

a negative regulator of podocyte differentiation pathways by inducing downregulation of WT1 and nephrin. The differences in gene expression seen in *Sema3a* deletion and overexpression models are remarkable in light of the paradoxical similarity of the morphologic podocyte changes. Epithelial cells are known to occasionally exhibit similar phenotypes upon gene knock-in and knockdown (Rogers et al., 2003); therefore, podocyte effacement might represent a final common pathway that occurs with disruption of podocyte differentiation.

The podocyte *Sema3a* overexpression phenotype strikingly resembles the *Lmx1b* gene deletion phenotype. *Lmx1b* is mutated in nail-patella syndrome, and gene deletion in mice results in cuboidal podocytes that lack foot processes and SDs, as well as glomerular hypoplasia with impaired glomerular capillary development (Miner et al., 2002; Rohr et al., 2002). Distinct differences between the two mouse models are the downregulation of WT1 and nephrin and lack of GBM phenotype in the newborn mice overexpressing podocyte *Sema3a*, whereas in *Lmx1b* knockouts, expression of these two podocyte proteins was not affected, podocin and VEGFA were downregulated and the GBM was abnormally expanded (Rohr et al., 2002). Dysregulation of *Sema3a* in newborn mice did not induce morphologic abnormalities in the GBM; however, defective GBM function and podocyte effacement might have contributed to the abnormal glomerular permeability observed in both models. The S*ema3a*-induced downregulation of VEGFR2 reported here could result in decreased VEGFA signaling, as was previously shown in cultured podocytes and in mice following systemic *Sema3a* administration (Guan et al., 2006; Tapia et al., 2008). Podocyte *Sema3a* overexpression induced mild podocyte apoptosis that did not alter podocyte number. This effect is consistent with, but of a lesser degree than, results previously described in vitro, and was likely attributable to a dose effect (Guan et al., 2006).

Semaphorin compensation

We identified *Sema3e* upregulation in *Sema3a*$^{-/-}$ mice. SEMA3E uniquely signals through plexin D1 (PLXND1) independently of neuropilins, and mutations in *Sema3e* are associated with CHARGE syndrome (Gu et al., 2005). *Sema3e* and *Plxnd1* gene deletion studies indicate that the ligand-receptor pair functions to restrict vessel growth and branching. Given the variability of vascular phenotypes of different strains of *Sema3a*$^{-/-}$ mice (Behar et al., 1996; Serini et al., 2003; Vieira et al., 2007), upregulation of *Sema3e* could provide an interesting mechanism by which compensation might occur in some *Sema3a*$^{-/-}$ mice.

In *Sema3a*-overexpressing mice, *Sema3b* was upregulated. SEMA3B binds to neuropilin 2 preferentially, antagonizes Sema3a-neuropilin-1 function on neurons, has been identified as an inhibitor of the AKT pathway and a tumor suppressor gene with loss of heterozygocity in lung, kidney and ovarian cancers (Castro-Rivera et al., 2004). The upregulation of *Sema3b* in response to *Sema3a* overexpression suggests a possible role for *Sema3b* in podocytes.

Semaphorins have been proposed as modulators of epithelial morphogenesis (Hinck, 2004), but no prior studies examined their role in glomerular development. The findings reported here provide in vivo evidence that *Sema3a* signaling is required for the regulation of renal vascular development and plays a crucial role in podocyte differentiation. Further study is warranted to determine the molecular mechanisms by which *Sema3a* interacts with *Pax2*, nephrin, *Wt1* and *Vegfr2* genes.

Supplementary material
Supplementary material for this article is available at
http://dev.biologists.org/cgi/content/full/136/22/3979/DC1

References
Abrahamson, D. R., Robert, B., Hyink, D. P., St John, P. L. and Daniel, T. O. (1998). Origins and formation of microvasculature in the developing kidney. *Kidney Int.* **Suppl. 67**, S7-S11.

Avner, E. D., Piesco, N. P., Sweeney, W. E., Jr and Ellis, D. (1988). Renal epithelial development in organotypic culture. *Pediatr. Nephrol.* **2**, 92-99.

Bagnard, D., Vaillant, C., Khuth, S. T., Dufay, N., Lohrum, M., Puschel, A. W., Belin, M. F., Bolz, J. and Thomasset, N. (2001). Semaphorin 3A-vascular endothelial growth factor-165 balance mediates migration and apoptosis of neural progenitor cells by the recruitment of shared receptor. *J. Neurosci.* **21**, 3332-3341.

Behar, O., Golden, J. A., Mashimo, H., Schoen, F. J. and Fishman, M. C. (1996). Semaphorin III is needed for normal patterning and growth of nerves, bones and heart. *Nature* **383**, 525-528.

Cai, Y., Brophy, P., Levitan, I., Stifani, S. and Dressler, G. (2003). Groucho suppresses Pax2 transactivation by inhibition of JNK-mediated phosphorylation. *EMBO J.* **22**, 5522-5529.

Castro-Rivera, E., Ran, S., Thorpe, P. and Minna, J. D. (2004). Semaphorin 3B (SEMA3B) induces apoptosis in lung and breast cancer, whereas VEGF165 antagonizes this effect. *Proc. Natl. Acad. Sci. USA* **101**, 11432-11437.

Davis, B., Dei Cas, A., Long, D. A., White, K. E., Hayward, A., Ku, C. H., Woolf, A. S., Bilous, R., Viberti, G. and Gnudi, L. (2007). Podocyte-specific expression of angiopoietin-2 causes proteinuria and apoptosis of glomerular endothelia. *J. Am. Soc. Nephrol.* **18**, 2320-2329.

Dehbi, M., Ghahremani, M., Lechner, M., Dressler, G. and Pelletier, J. (1996). The paired-box transcription factor, PAX2, positively modulates expression of the Wilms' tumor suppressor gene (WT1). *Oncogene* **13**, 447-453.

Done, S. C., Takemoto, M., He, L., Sun, Y., Hultenby, K., Betsholtz, C. and Tryggvason, K. (2008). Nephrin is involved in podocyte maturation but not survival during glomerular development. *Kidney Int.* **73**, 697-704.

Eremina, V., Sood, M., Haigh, J., Nagy, A., Lajoie, G., Ferrara, N., Gerber, H. P., Kikkawa, Y., Miner, J. H. and Quaggin, S. E. (2003). Glomerular-specific alterations of VEGF-A expression lead to distinct congenital and acquired renal diseases. *J. Clin. Invest.* **111**, 707-716.

Gerber, H. P., Hillan, K. J., Ryan, A. M., Kowalski, J., Keller, G. A., Rangell, L., Wright, B. D., Radtke, F., Aguet, M. and Ferrara, N. (1999). VEGF is required for growth and survival in neonatal mice. *Development* **126**, 1149-1159.

Gu, C., Rodriguez, E. R., Reimert, D. V., Shu, T., Fritzsch, B., Richards, L. J., Kolodkin, A. L. and Ginty, D. D. (2003). Neuropilin-1 conveys semaphorin and VEGF signaling during neural and cardiovascular development. *Dev. Cell* **5**, 45-57.

Gu, C., Yoshida, Y., Livet, J., Reimert, D. V., Mann, F., Merte, J., Henderson, C. E., Jessell, T. M., Kolodkin, A. L. and Ginty, D. D. (2005). Semaphorin 3E and plexin-D1 control vascular pattern independently of neuropilins. *Science* **307**, 265-268.

Guan, F., Villegas, G., Teichman, J., Mundel, P. and Tufro, A. (2006). Autocrine class 3 semaphorin system regulates slit diaphragm proteins and podocyte survival. *Kidney Int.* **69**, 1564-1569.

Guo, G., Morrison, D. J., Licht, J. D. and Quaggin, S. E. (2004). WT1 activates a glomerular-specific enhancer identified from the human nephrin gene. *J. Am. Soc. Nephrol.* **15**, 2851-2856.

Guo, J. K., Menke, A. L., Gubler, M. C., Clarke, A. R., Harrison, D., Hammes, A., Hastie, N. D. and Schedl, A. (2002). WT1 is a key regulator of podocyte function: reduced expression levels cause crescentic glomerulonephritis and mesangial sclerosis. *Hum. Mol. Genet.* **11**, 651-659.

Guttmann-Raviv, N., Shraga-Heled, N., Varshavsky, A., Guimaraes-Sternberg, C., Kessler, O. and Neufeld, G. (2007). Semaphorin-3A and semaphorin-3F work together to repel endothelial cells and to inhibit their survival by induction of apoptosis. *J. Biol. Chem.* **282**, 26294-26305.

Harper, S. J., Xing, C. Y., Whittle, C., Parry, R., Gillatt, D., Peat, D. and Mathieson, P. W. (2001). Expression of neuropilin-1 by human glomerular epithelial cells in vitro and in vivo. *Clin. Sci.* **101**, 439-446.

He, Z. and Tessier-Lavigne, M. (1997). Neuropilin is a receptor for the axonal chemorepellent Semaphorin III. *Cell* **90**, 739-751.

Hinck, L. (2004). The versatile roles of "axon guidance" cues in tissue morphogenesis. *Dev. Cell* **7**, 783-793.

Hirose, K., Osterby, R., Nozawa, M. and Gundersen, H. J. (1982). Development of glomerular lesions in experimental long-term diabetes in the rat. *Kidney Int.* **21**, 689-695.

Ji, J. D., Park-Min, K. H. and Ivashkiv, L. B. (2009). Expression and function of semaphorin 3A and its receptors in human monocyte-derived macrophages. *Hum. Immunol.* **70**, 211-217.

Karihaloo, A., Karumanchi, S. A., Cantley, W. L., Venkatesha, S., Cantley, L. G. and Kale, S. (2005). Vascular endothelial growth factor induces branching morphogenesis/tubulogenesis in renal epithelial cells in a neuropilin-dependent fashion. *Mol. Cell. Biol.* **25**, 7441-7448.

Kawasaki, T., Kitsukawa, T., Bekku, Y., Matsuda, Y., Sanbo, M., Yagi, T. and Fujisawa, H. (1999). A requirement for neuropilin-1 in embryonic vessel formation. *Development* **126**, 4895-4902.

Kestila, M., Lenkkeri, U., Mannikko, M., Lamerdin, J., McCready, P., Putaala, H., Ruotsalainen, V., Morita, T., Nissinen, M., Herva, R. et al. (1998). Positionally cloned gene for a novel glomerular protein-nephrin-is mutated in congenital nephrotic syndrome. *Mol. Cell* **1**, 575-582.

Kitamoto, Y., Tokunaga, H. and Tomita, K. (1997). Vascular endothelial growth factor is an essential molecule for mouse kidney development: glomerulogenesis and nephrogenesis. *J. Clin. Invest.* **99**, 2351-2357.

Kitsukawa, T., Shimono, A., Kawakami, A., Kondoh, H. and Fujisawa, H. (1995). Overexpression of a membrane protein, neuropilin, in chimeric mice causes anomalies in the cardiovascular system, nervous system and limbs. *Development* **121**, 4309-4318.

Kolodkin, A. L., Levengood, D. V., Rowe, E. G., Tai, Y. T., Giger, R. J. and Ginty, D. D. (1997). Neuropilin is a semaphorin III receptor. *Cell* **90**, 753-762.

Kreidberg, J. A., Donovan, M. J., Goldstein, S. L., Rennke, H., Shepherd, K., Jones, R. C. and Jaenisch, R. (1996). Alpha 3 beta 1 integrin has a crucial role in kidney and lung organogenesis. *Development* **122**, 3537-3547.

Laitinen, L. (1987). Griffonia simplicifolia lectins bind specifically to endothelial cells and some epithelial cells in mouse tissues. *Histochem. J.* **19**, 225-234.

Lindahl, P., Hellstrom, M., Kalen, M., Karlsson, L., Pekny, M., Pekna, M., Soriano, P. and Betsholtz, C. (1998). Paracrine PDGF-B/PDGF-Rbeta signaling controls mesangial cell development in kidney glomeruli. *Development* **125**, 3313-3322.

Little, M., Holmes, G., Bickmore, W., van Heyningen, V., Hastie, N. and Wainwright, B. (1995). DNA binding capacity of the WT1 protein is abolished by Denys-Drash syndrome WT1 point mutations. *Hum. Mol. Genet.* **4**, 351-358.

Lobe, C. G., Koop, K. E., Kreppner, W., Lomeli, H., Gertsenstein, M. and Nagy, A. (1999). Z/AP, a double reporter for cre-mediated recombination. *Dev. Biol.* **208**, 281-292.

McConnell, M. J., Cunliffe, H. E., Chua, L. J., Ward, T. A. and Eccles, M. R. (1997). Differential regulation of the human Wilms tumour suppressor gene (WT1) promoter by two isoforms of PAX2. *Oncogene* **14**, 2689-2700.

Miao, H. Q., Soker, S., Feiner, L., Alonso, J. L., Raper, J. A. and Klagsbrun, M. (1999). Neuropilin-1 mediates collapsin-1/semaphorin III inhibition of endothelial cell motility: functional competition of collapsin-1 and vascular endothelial growth factor-165. *J. Cell Biol.* **146**, 233-242.

Miner, J. H. and Li, C. (2000). Defective glomerulogenesis in the absence of laminin alpha5 demonstrates a developmental role for the kidney glomerular basement membrane. *Dev. Biol.* **217**, 278-289.

Miner, J. H., Morello, R., Andrews, K. L., Li, C., Antignac, C., Shaw, A. S. and Lee, B. (2002). Transcriptional induction of slit diaphragm genes by Lmx1b is required in podocyte differentiation. *J. Clin. Invest.* **109**, 1065-1072.

Moretti, S., Procopio, A., Lazzarini, R., Rippo, M. R., Testa, R., Marra, M., Tamagnone, L. and Catalano, A. (2008). Semaphorin3A signaling controls Fas (CD95)-mediated apoptosis by promoting Fas translocation into lipid rafts. *Blood* **111**, 2290-2299.

Putaala, H., Soininen, R., Kilpelainen, P., Wartiovaara, J. and Tryggvason, K. (2001). The murine nephrin gene is specifically expressed in kidney, brain and pancreas: inactivation of the gene leads to massive proteinuria and neonatal death. *Hum. Mol. Genet.* **10**, 1-8.

Quaggin, S. E. and Kreidberg, J. A. (2008). Development of the renal glomerulus: good neighbors and good fences. *Development* **135**, 609-620.

Robert, B., Zhao, X. and Abrahamson, D. R. (2000). Coexpression of neuropilin-1, Flk1, and VEGF(164) in developing and mature mouse kidney glomeruli. *Am. J. Physiol. Renal. Physiol.* **279**, F275-F282.

Rogers, K. K., Jou, T. S., Guo, W. and Lipschutz, J. H. (2003). The Rho family of small GTPases is involved in epithelial cystogenesis and tubulogenesis. *Kidney Int.* **63**, 1632-1644.

Rohr, C., Prestel, J., Heidet, L., Hosser, H., Kriz, W., Johnson, R. L., Antignac, C. and Witzgall, R. (2002). The LIM-homeodomain transcription factor Lmx1b plays a crucial role in podocytes. *J. Clin. Invest.* **109**, 1073-1082.

Ryan, G., Steele-Perkins, V., Morris, J. F., Rauscher, F. J., 3rd. and Dressler, G. R. (1995). Repression of Pax-2 by WT1 during normal kidney development. *Development* **121**, 867-875.

Sariola, H. (1984). Incomplete fusion of the epithelial and endothelial basement membranes in interspecies hybrid glomeruli. *Cell Differ.* **14**, 189-195.

Schmittgen, T. D. and Livak, K. J. (2008). Analyzing real-time PCR data by the comparative C(T) method. *Nat. Protoc.* **3**, 1101-1108.

Serini, G., Valdembri, D., Zanivan, S., Morterra, G., Burkhardt, C., Caccavari, F., Zammataro, L., Primo, L., Tamagnone, L., Logan, M. et al. (2003). Class 3 semaphorins control vascular morphogenesis by inhibiting integrin function. *Nature* **424**, 391-397.

Shalaby, F., Rossant, J., Yamaguchi, T. P., Gertsenstein, M., Wu, X. F., Breitman, M. L. and Schuh, A. C. (1995). Failure of blood-island formation and vasculogenesis in Flk-1-deficient mice. *Nature* **376**, 62-66.

Shigehara, T., Zaragoza, C., Kitiyakara, C., Takahashi, H., Lu, H., Moeller, M., Holzman, L. B. and Kopp, J. B. (2003). Inducible podocyte-specific gene expression in transgenic mice. *J. Am. Soc. Nephrol.* **14**, 1998-2003.

Takemoto, M., He, L., Norlin, J., Patrakka, J., Xiao, Z., Petrova, T., Bondjers, C., Asp, J., Wallgard, E., Sun, Y. et al. (2006). Large-scale identification of genes implicated in kidney glomerulus development and function. *EMBO J.* **25**, 1160-1174.

Tamagnone, L., Artigiani, S., Chen, H., He, Z., Ming, G. I., Song, H., Chedotal, A., Winberg, M. L., Goodman, C. S., Poo, M. et al. (1999). Plexins are a large family of receptors for transmembrane, secreted, and GPI-anchored semaphorins in vertebrates. *Cell* **99**, 71-80.

Tapia, R., Guan, F., Gershin, I., Teichman, J., Villegas, G. and Tufro, A. (2008). Semaphorin3a disrupts podocyte foot processes causing acute proteinuria. *Kidney Int.* **73**, 733-740.

Torres, M., Gomez-Pardo, E., Dressler, G. R. and Gruss, P. (1995). Pax-2 controls multiple steps of urogenital development. *Development* **121**, 4057-4065.

Tufro, A. (2000). VEGF spatially directs angiogenesis during metanephric development in vitro. *Dev. Biol.* **227**, 558-566.

Tufro, A., Norwood, V. F., Carey, R. M. and Gomez, R. A. (1999). Vascular endothelial growth factor induces nephrogenesis and vasculogenesis. *J. Am. Soc. Nephrol.* **10**, 2125-2134.

Tufro, A., Teichman, J., Woda, C. and Villegas, G. (2008). Semaphorin3a inhibits ureteric bud branching morphogenesis. *Mech. Dev.* **125**, 558-568.

Tufro-McReddie, A., Norwood, V. F., Aylor, K. W., Botkin, S. J., Carey, R. M. and Gomez, R. A. (1997). Oxygen regulates vascular endothelial growth factor-mediated vasculogenesis and tubulogenesis. *Dev. Biol.* **183**, 139-149.

Vieira, J. M., Schwarz, Q. and Ruhrberg, C. (2007). Selective requirements for NRP1 ligands during neurovascular patterning. *Development* **134**, 1833-1843.

Villegas, G. and Tufro, A. (2002). Ontogeny of semaphorins 3A and 3F and their receptors neuropilins 1 and 2 in the kidney. *Mech. Dev.* **119**, **Suppl. 1**, S149-S153.

Wagner, K., Wagner, N., Guo, J., Elger, M., Dallman, M., Bugeon, L. and Schedl, A. (2006). An inducible mouse model for PAX2-dependent glomerular disease: insights into a complex pathogenesis. *Curr. Biol.* **16**, 793-800.

Wagner, N., Wagner, K. D., Xing, Y., Scholz, H. and Schedl, A. (2004). The major podocyte protein nephrin is transcriptionally activated by the Wilms' tumor suppressor WT1. *J. Am. Soc. Nephrol.* **15**, 3044-3051.